***Original Research Article***

# Influence of Spin Coating Speed on Optical Properties of Spin-Coated $TiO_2$ Thin Films.


## ABSTRACT

In this work, nanocrystalline $TiO_2$thin films have been prepared by the sol-gel spin coating method at different spin speeds. X-ray diffraction (XRD), Scanning electron microscopy, and UV–vis spectroscopy were used to investigate the structural and optical properties of the deposited thin films. After the deposition, the samples were annealed in the open air and under the microwave. The results showed an optical energy gap of 3.33-3.61 eV for direct transition for the samples annealed in the open air and 3.28-3.48 eV for samples annealed under the microwave. Indirect transition on the other hand stood at 3.99 eV for all the 3 samples annealed in open air and 3.84-3.91eV for samples annealed under microwave respectively. This work has shown that annealing either in open air or in a microwave can influence the structural and optical properties of thin films of $TiO_2$. Other optical parameters studied include optical transmittance, refractive index, reflectance, absorbance dielectric constants, etc.



*Keywords: Open-air annealing, Microwave annealing, titanium oxide, XRD, FE-SEM*


## 1. INTRODUCTION

Titanium dioxide ($TiO_2$), commonly known as titanium oxide or titania, is a widely studied material in the realm of nanotechnology and thin film technology. Its excellent optical properties, coupled with its high chemical stability and biocompatibility (Stoyanova et al., 2017, Abbas and Bensaha, 2021), have led to its extensive utilization in fields such as photovoltaics, photocatalysis, resistive switching applications such as random-access memory, neuromorphic computing, biohybrid interfaces, and sensors and in optical coatings (Georgii et al., 2020, Noman et al., 2019, Soussi et al., 2021, Elshahawy et al., 2023). The unique optical properties of $TiO_2$ thin films arise from the complex interaction of light with its crystalline structure and electronic transitions. As a highly transparent material in the visible spectrum with a wide bandgap of around 3.2 eV, $TiO_2$ exhibits a significant refractive index and low extinction coefficient in the ultraviolet (UV) range, making it desirable for applications requiring UV light manipulation (Manickam et al., 2019). Titanium (IV) dioxide (titania) exists in three common crystalline phases: rutile, which is the thermodynamically stable phase, and the metastable phases anatase and brookite. Anatase and rutile have more extensive applications because they are more stable than brookite (Scarpelli et al., 2018, Lias et al., 2016, Promnopas et al., 2016). The crystal phase can be tailored through deposition techniques, allowing for precise control over the material's optical properties to suit specific applications.

There are many techniques for the synthesis of Titanium dioxide or Titania ($TiO_2$) thin films, such as the soll-gel technique (Adawiya et al., 2017, Mohd et al., 2016, Sabry et al., 2016, Karoui et al., 2015, Obregón et al., 2022, Min, H 2021, Rahmani and Ardyanian, 2018), electro-deposition (Dohyun-Go et al., 2021), spin coating [Soussi et al., 2021), chemical vapor deposition (Reinke et al., 2015), laser deposition (Ishii et al., 2015), atomic layer method (Jolivet., 2023), hydrothermal method (Kumara et al., 2018), thermal evaporation technique (El-Nahass et al., 2018), spray pyrolysis (Hamid et al., 2019) and reactive sputtering techniques (Daughtry et al., 2021, Hajjaji et al., 2015).

The spin-coating method is interesting because it involves two steps to produce thin films of various semiconductors; first, a sol-gel of the precursor solution is prepared, and then the desired material is deposited onto a substrate using the spin - coating technique (Engberg et al., 2020, Ahmoum et al., 2020, Özdal et al., 2020, Abdellatif et al., 2018).

In order to offer insightful information on the fundamental behavior of $TiO_2$thin films under various experimental circumstances, we present a thorough investigation into their optical properties in this paper. The work includes experimental data gathered using spectroscopic methods, providing a fresh understanding of how TiO2 thin films behave under varied spin speeds.

## 2. EXPERIMENTAL DETAILS

To make the precursor solution, 3 grams of $TiO_2$ powder of 99.99% purity from Sigma Aldrich were measured and dissolved in 25 ml of ethanol. The resulting solution was stirred for 30 minutes using a magnetic stirrer at room temperature in an airtight container. A spin coater (Model WS-650MZ-23NPP) was used to spin the substrate at various speeds ranging from 500 to 2500 rpm with a spin time of 30 seconds for each film after dispensing about 2.0 µl of the spreading solution onto the glass substrate maintaining a distance of approximately 5.0 mm between the dispenser and the substrate. Prior to the deposition, the glass slides (corning)used as the substrates (25.4 mm × 76.2 mm) were washed with detergent solution for 10 to 15 minutes in an ultrasonic Sonicator and rinsed in distilled water for 15 minutes at room temperature (RT). The substrates were later cleaned with Isopropanol Alcohol (IPA) in the ultrasonic bath for 15 minutes at room temperature and dried in a stream of nitrogen gas (N2). Three of the six samples produced (A500, A1500, and A2500) were annealed in a Carbolite horizontal furnace in the open air at $100^0$C for 1 hour and then slowly cooled to room temperature. The remaining three samples (MWA 500, MWA 1500, and MWA 2500) were subjected to microwave annealing (MWA) by mounting the samples onto a Silicon Carbide (SiC) susceptor. The frequency, power, and time for the MWA were set at 2.45 GHz, 800W, and 2.5 minutes respectively. The structural properties of the samples were studied by X-ray diffractometer (Minflex 300/600). The diffractometer operated on 40kv and 15mA is having Cukα radiation (λ=1.5418 Angstroms). The diffraction angle was between 20 and 700 with a scanning rate of 100/minute and a 2θ step width of 0.010. The surface morphology was analyzed by FE-SEM. The optical properties of all the samples were recorded by UV-VIS-NIR spectrophotometer (Avaspec 2048). To cover both the visible and the infrared range of the spectrum, the wavelength region was set between 190nm to 1100nm. Veeco Dektak profile meter was used to determine the thickness, surface roughness, and radius of curvature of the samples. The thickness of the thin films was estimated at 185 nm.

## 3. RESULTS AND DISCUSSION

### 3.1 Structural Properties

The XRD patterns of the $TiO_2$ thin films annealed in open air and under microwave were shown in Figure 1 (a and b). The Figure reveals tetragonal anatase and rutile crystal structures with sharp and broad peaks (matching ICDD cards no. 96-900-8215 and 96-900-4143). The tetragonal anatase phase peaked at 2 Theta degrees of 25.27, 37.70, 47.98, 53.76, and 54.99 related to (hkl) crystal levels of (101), (004), (200), (105) and (211) respectively. The sample deposited at a spin speed of 1500 (A1500) also shows both anatase and rutile phases with planes of reflections (004), (105) and (211) observed in sample A500 disappearing. In this sample, the lone rutile phase located at 2 Theta 62.80 is related to the (hkl) crystal level of (002). The X-ray diffractogram of $TiO_2$ thin films grown at a spin speed of 2500 and annealed in open air (A2500) is also shown in Figure 1 (a). The sample is observed to have preferential crystallographic structure texture in the (101), (004), (200) and (211) directions corresponding to the Bragg's angles 2θ=25.33, 37.81, 48.10, and 55.14 found in ICDD card number 96-900-8215 for the anatase phase. The sample also has the rutile phases located at 2θ=54.19 and 62.58 at hkl (211) and (002).

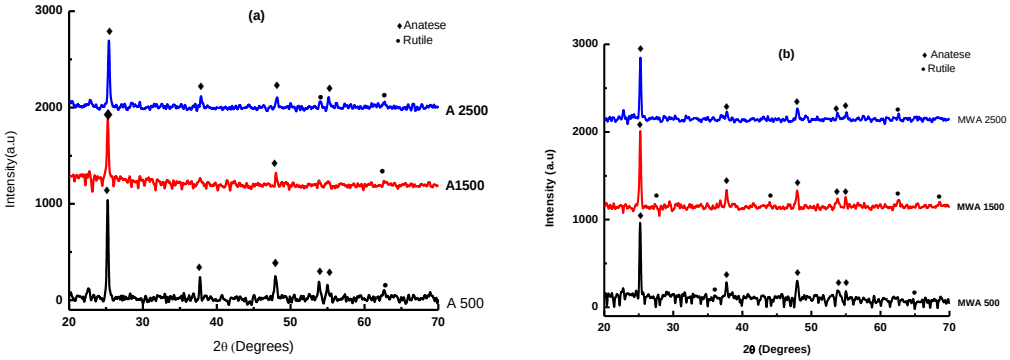


**Fig. 1. XRD diffraction patterns for TiO2 thin films annealed in open and under Microwave**

XRD patterns of $TiO_2$ thin films grown at different spin speeds and annealed under microwave are presented in Figure 1 (b). All the samples (MWA 500, 1500, and 2500) have confirmed anatase and rutile (tetragonal) phases. In all the samples, up to 5 peaks of the anatase phase have been identified and located at 2θ= 25.21, 37.53, 47.88, 51.76, and 54.87 with (101), (004), (200), (105), and (211) planes of reflections referenced with ICDD card number 96-900-8215 and 96-900-8216. Rutile phases of hkl (101) and (002) at 2θ= 36.01 and 62.80 have been detected in the sample spun at 500 rpm. Four rutile phases appeared for sample MWA 1500 located at hkl (110), (210), (310), and (301) at 2θ= 27.26, 43.75, 62.12, and 68.46. The only rutile phase observed in sample MWA 2500 is located at 2θ=64.07 and hkl (310). All the rutile phases are referenced with ICDD card number 96-900-4143. The appearance of more peaks of the anatase phase in the spectra of the samples confirmed that deposition at higher speeds can improve crystallinity. The appearance of the rutile phase on the other hand can be related to annealing which can create enough energy transformation to effect phase transformation (Lukong et al., 2021). Furthermore, higher spin speed may promote denser packing which can improve crystal

### 3.2 Optical Transmittance

Figure 2 (a and b) shows the spectral transmittance of the thin films of $TiO_2$ annealed in open air at $100^0$C for 1 hour. The transmittance of the samples increases with an increase in the number of revolutions of the spin coater.

As known, film thickness directly influences optical properties such as transparency and absorption. Thinner films resulting from higher spin speeds might have lower absorption and higher transparency in some cases. However, if the film becomes too thin, issues with light scattering and incomplete coverage might be encountered. The increase in transmittance in thin films is attributed to the reduction in the thickness of the film. The decrease in transmittance on the other hand is related to the semiconducting nature of $TiO_2$ due to the existence of a large band gap. Materials that absorb UV radiation and possess high transmittance in the visible range can be used as protection for optoelectronic devices against UV radiation (Khan et al., 2017). Transmittance can be calculated from Equation (1) given by (Dai et al., 2019).

$$R+T+A=1 \quad (1)$$

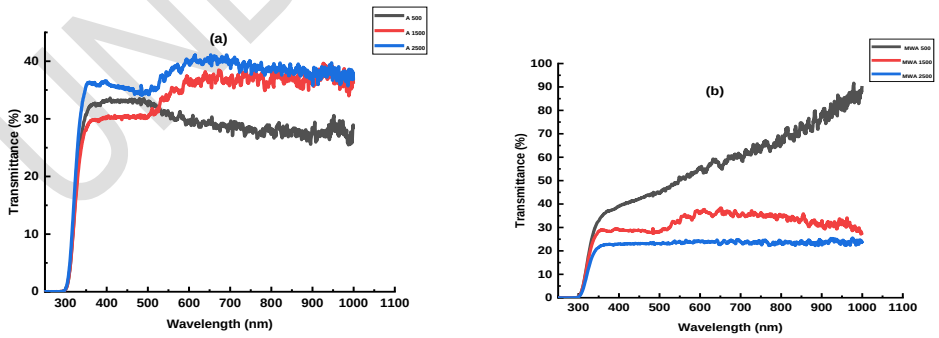


**Fig. 2. Transmittance for samples annealed in open air and under Microwave**

Transmittance for $TiO_2$ thin films annealed under microwave is also shown in Figure 2 (b). It can be seen that the transmittance of all the samples decreased if compared with those annealed in open air. This shows that these samples are more absorbable than those annealed in open air. This behavior may be a result of condensation of oxygen during the annealing process. A decrease in transmittance may be a result of light absorption caused by the excitation and migration of electrons from the valence to the conduction band (Al-Jawad et al., 2017).

Generally, an increase in transmittance for thin films can also be related to the fact that the roughness of the samples increases as a result of annealing. This roughness causes scattering. Annealing can also result in larger grain size which may improve transmittance (Taha et al., 2017). Lower-level defects acting as scattering centers can also result in an increase in transmittance.

### 3.3 Optical band gap

Figure 3 (a and b) represents the direct optical band gap of $TiO_2$ thin films. These band gaps were calculated from Tauc's relation given as Equation (2) by (Abdullahi et al., 2017).

$$(\alpha h\nu) = A(h\nu - E_g)^n \qquad (2)$$

Where hv is the photon energy, A is a constant, and n is equal to 0.5 and 2 for direct and indirect electron transitions. The linear variation of $(\alpha h\nu)^2$ vs hv at the absorption edge confirmed that these films are semiconducting. Extrapolating the straight-line portion of the plot $(\alpha h\nu)^2$ vs hv for zero absorption coefficient (α) value gives the optical band gap ($E_g$). The direct optical band gap for samples A 500 and A 1500 is 3.61 eV and 3.33 eV for A 2500. For samples MWA 500 and MWA 1500, the band gap is 3.48 eV and 3.28 eV for sample MWA 2500 respectively. The band gap obtained for A 2500 and MWA 2500 is very close to that obtained by (Karoui et al., 2015). The band gap determined for sample MWA 500 was also reported by (Alaya et al., 2023).

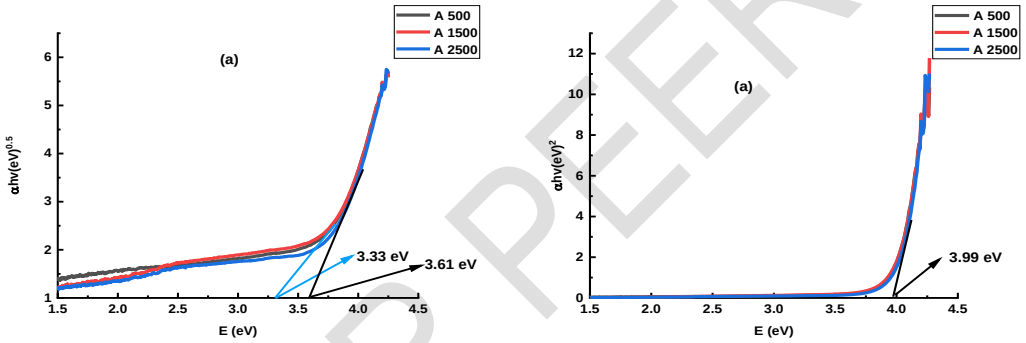


**Fig. 3. Direct Band Gap Energy for samples annealed open air and under Microwave**

Figure 4 (a and b) shows the indirect band gap for $TiO_2$ thin films annealed in the open air and under the microwave. The indirect band gap for all the 3 samples annealed in open air is 3.99 eV and 3.91 for samples MWA 500 and MWA 1500 and 3.84 for sample MWA 2500 respectively.

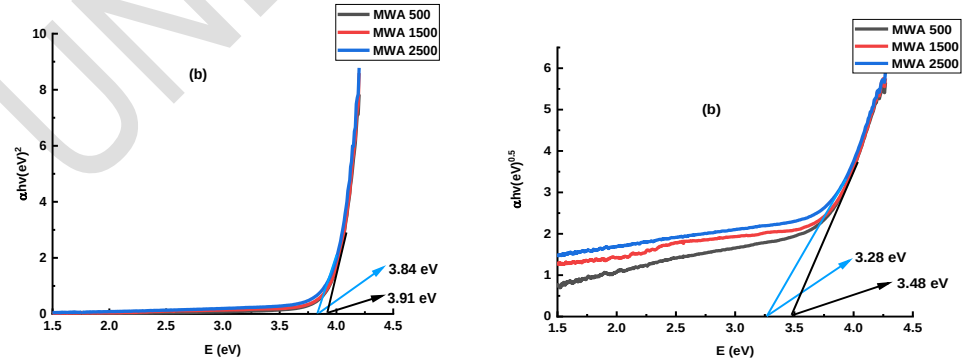


Fig. 4. Indirect Band Gap Energy for samples annealed open air and under Microwave

It is worthy of note that $TiO_2$ has both direct and indirect band gaps. The increase in both direct and indirect band gaps is related to the increase in the number of charge carrier probabilities resulting from annealing. This increase can also be a result of changes in grain size and modified carrier concentration (Taha et al., 2017 and Rajesh, 2017). According to Zharvan et al., 2016, the energy gap of thin films TiO increases can be attributed to the size of the crystal. The larger size of anatase crystals will provide a lower energy gap. This phenomenon is well-known as a quantum size effect. This effect is known to have an important role in controlling the photochemical properties and photocatalytic of semiconductor materials. As can be seen in Figure 4 (a and b), the $E_g$ varies for the two regimes of samples indicating that the films can be used as window material for thin film solar cells. It has been observed that the E_g varies with an increase in spin speed. This spin speed causes uniform spreading of the material on the substrate exhibiting a more ordered structure by covering the number of defects which causes less contribution to absorption (Rajesh, 2017). A decrease in band gap energy is related to the transformation from anatase to rutile phase and increased crystallinity (Lukong et al., 2021).

### 3.4 Refractive index (n)

Figure 5 (a and b) shows the refractive indices for all six samples. As stated earlier, spin speed influences thin film properties such as transparency and absorption which are directly related to the refractive index (n). The refractive index can be calculated from Equation (3) given by (Hassanien and El Radaf, 2020).

$$n = \frac{1+R}{1-R} + \left(\frac{4R}{(1-R)^2} + k^2\right)^{1/2} \quad (3)$$


Fig. 5. Refractive index for samples annealed in open air and under Microwave

For the samples annealed under the microwave, n increases with an increase in spin speed for samples MWA1500 and MWA2500 respectively. An increase in the refractive index may be attributed to higher packing density resulting from the annealing because a change in crystalline structure may cause a change in the refractive index.

Furthermore, a decrease in the refractive index shows a normal semiconducting behavior of the material. An increase in the volume fraction of voids available on the film surface also causes a decrease in the refractive index (Dizaji et al., 2011).

### 3.5 Absorption coefficient (α)

Figure 6 (a and b) shows the absorption coefficient (α) of the $TiO_2$ thin films annealed in open air and under a microwave oven. The thin films were grown at different spin speeds ranging from 500 to 2500 rpm. The absorption coefficient was determined from absorbance measurements using Equation (4) by (Abdullahi et al., 2020).

$$\alpha = \frac{1}{d} \ln \frac{(1-R)^2}{T} \quad (4)$$

where d is the film thickness, r is the reflectance, and t is the transmittance

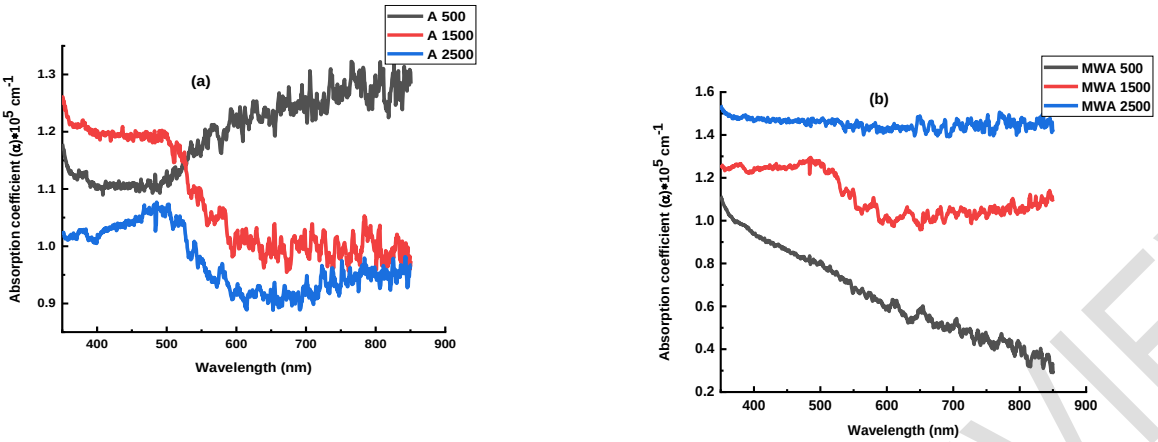


Fig. 6. Absorption coefficient for samples annealed in the open air and under Microwave

The absorption coefficient is above $10^5 \mathrm{cm}^{-1}$ for all the samples indicating that all the samples have the property to absorb photons. It has been observed that the absorption coefficient increases with spin speed which can be linked to the improvement in the crystallinity resulting from annealing.

### 3.6 Dielectric constant

As the quantity that measures the ability of a material to store electrical energy in an electric field, the real ($\varepsilon_r$) and imaginary ($\varepsilon_i$) parts of the dielectric constant that can be expressed as Equations (5) and (6) from (Hassanien and El Radaf, 2020) is presented in Figures 7 (a and b) and 8 (a and b).

$$\varepsilon_r = n^2 - k^2 \quad (5)$$

$$\varepsilon_i = 2nk \quad (6)$$

The real part shown in Figure 7 (a and b) varied with spin speed such a pattern has also been observed for the refractive index.

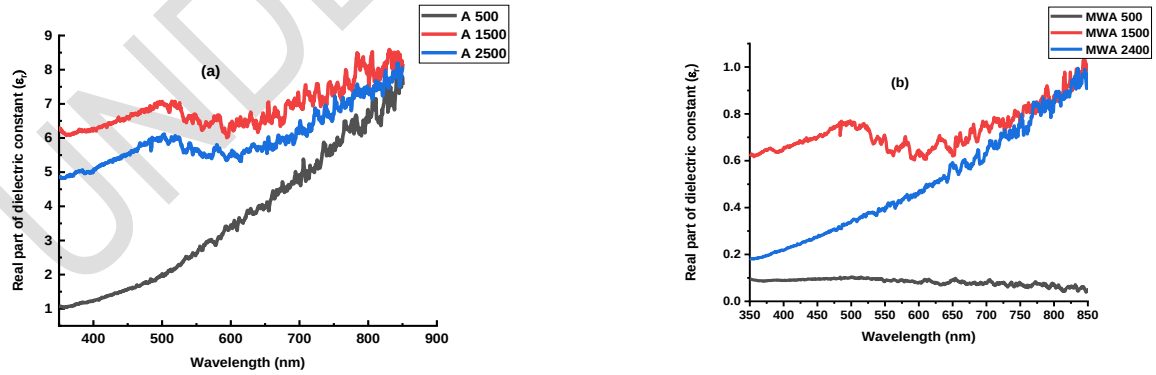


Fig. 7. Real part of the dielectric constant for samples annealed in open air and under Microwave

The imaginary part shown in Figure 8 (a and b) on the other hand shows a strong relationship between ($\varepsilon_i$) and the extinction coefficient (k). There are noticeable increases in both real and imaginary parts of the refractive index with an increase in spin speed. This shows a good optical response of the samples.

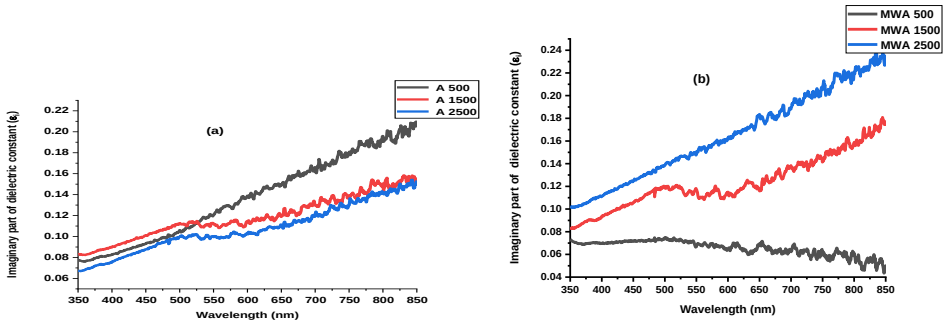


Fig. 8. Imaginary part of the dielectric constant for samples annealed in open air and under Microwave

## 4. CONCLUSION

In conclusion, high-quality TiO2 thin films were deposited on a glass substrate via the spin coating method and annealed in the open air and under the microwave. Their optical properties with respect to spin speed were investigated. X-ray diffraction analysis showed the existence of both anatase and rutile crystal structures. In addition, the transmittance, absorbance, and energy band gap of the samples within the visible region varied according to the spin speed. These properties make it useful for many applications such as antireflection coating, self-cleaning glass, gas sensors, dielectric materials, etc. Finally, these TiO2 thin films may be a potential candidate in optoelectronics devices due to their attractive optical properties.

## REFERENCES


1. Stoyanova D, Ivanova I, Angelov O and Vladkova T. Antibacterial activity of thin films $TiO_2$ doped with Ag and Cu on Gracilicutes and Firmicutes bacteria. Biodiscovery 2017; e21596.https://doi.org/10.3897/biodiscovery.20.e21596

2. Abbas F and Bensaha R. Effect of annealing time on structural and optical proprieties of mercury ($Hg^{+2}$) doped $TiO_2$ thin films elaborated by sol-gel method for future photo-catalytic application. Optik. 2021; (247), 167846

3. Georgii A, Illarionov G, Morozova S. M, Christoph V V, Einarsrud M, Morozov M I. Memristive $TiO_2$: Synthesis, Technologies, and Applications, Front. Chem 2020; 8 – 2020. https://doi.org/10.3389/fchem.2020.00724

4. Noman MT, Ashraf MA, and Ali A. Synthesis and applications of nano-$TiO_2$: a review. Environ Sci Pollut Res. 2019; 26 :3262–3291. https://doi.org/10.1007/s11356-018-3884-z

5. Soussi A, AitHssi A, Boujnah M. Electronic and Optical Properties of $TiO_2$ Thin Films: Combined Experimental and Theoretical Study. Journal of Electron Mater. 2021; 50: 4497–4510. https://doi.org/10.1007/s11664-021-08976-8

6. Elshahawy, A M, Elkatlawy S. M,Shalaby M. S,Guan C and Wang J. Surface-Engineered $TiO_2$for High-Performance Flexible Supercapacitor Applications. J Electron Mater. 2023; 52 :1347–1356

7. Manickam K, Muthusamy V, Manickam S, Senthil T.S, Periyasamy G, and Shanmugam S. Effect of annealing temperature on structural, morphological, and optical properties of nanocrystalline $TiO_2$thin films synthesized by sol–gel dip coating method. Mater Today 2019; Proceedings xxx (xxxx) xxx. https://doi.org/10.1016/j.matpr.2019.06.651

8. Scapelli, F, Mastropietro, T F, Poerio T and Godbert N (2018). Mesoporous $TiO_2$Thin Films: State of the Art. in: Titanium Dioxide - Material for a Sustainable Environment. InTech; 2018. http://dx.doi.org/ 10.5772/intechopen.74244

9. Lias J, Shahadan SA, Rahim MSA, Nayan N, Ahmad MK and Sahdan MZ. Influences of Deposition time on $TiO_2$ Thin films properties prepared by CVD technique. JurnalTeknologi (Sciences & Engineering). 2016; 78: 10–3: 1–5

10. Promnopas W, Promnopas S, Phonkhokkong T, Thongtem T, Boonyawan D, Yu L, Wiranwetchayan O, Phuruangrat A, Thongtem S. Crystalline phases and optical properties of titanium dioxide films deposited on glass substrates by microwave method. Surf and Coat Technol. 2016; 306, Part A: 69-74. doi.org/10.1016/j.surfcoat.2016.04.078.

11. Adawiya J, Riyad H. A, Ghadah RK and Chafic TS. Exploring potential Environmental applications of $TiO_2$. Energy Procedia. 2017; 119:332–345.

12. Mohd SND, Sahdan MZ, Senain I, Bakri AS, Abdullah SA, Mokhter F, Ahmad A and Saim H. Preparation, Characterization, and Morphological study of Co–doped$TiO_2$ Thin Films. J. Engineering and Applied Sciences. 2016; 11(8):4924- 4928.

13. Sabry R. S, Al-Haidarie Y. K and Kudhier, M A. Synthesis and photocatalytic activity of $TiO_2$ nanoparticles prepared by sol–gel method. J Solgel Sci Technol 2016. 78 (2016): 299-306.

14. Karoui B.Z, Kaddachi M and Gharbi R. Optical properties of nanostructured $TiO_2$ thin films. J Phys Conf Ser 2015; 596 (2015) 1212

15. Obregón S and Rodríguez-González V. Photocatalytic $TiO_2$ thin films, and coatings prepared by sol–gel processing: a brief review. J Sol-Gel Sci Technol. 2022; 102: 125–141. https://doi.org/10.1007/s10971-021-05628-5

16. Min, Ho. Thin films deposited by spin coating technique: review. Pak J Chem. 2021; 11: 38-47. 10.15228/2021.v11. 103-407.

17.Rahmani, F and Ardyanian, M. Fabrication and characterization of ZnO/$TiO_2$ multilayers, deposited via spin coating method. J Mater Sci: Mater Electron. 2018; 29: 4285–4293 (2018). https://doi.org/10.1007/s10854-017-8375-3

18. Dohyun Go D, Lee J, Shin JW, Lee S, Kang W, Han JH, Jihwan. A Phase-gradient atomic layer deposition of $TiO_2$ thin films by plasma-induced local crystallization. Ceram Int. 2021; 47 (20): 28770-28777

19. Reinke M, Ponomarev E, Kuzminykh Y and Hoffmann P. Combinatorial characterization of $TiO_2$ chemical vapor deposition utilizing titanium isopropoxide. ACS Comb Scie. 2015; 17(7):413- 420.

20. Ishii A, Nakamura Y, Oikawa I, Kamegawa A and Takamura H. Magnesium Doping for the Promotion of Rutile Phase Formation in the Pulsed Laser Deposition of $TiO_2$ Thin Films. Appl Surf Sci. 2015; 347:528–534.

21. Jolivet A, Labbé C, Frilay C, Debieu O, Marie P, Horcholle B, Lemarié F, Portier X, Grygiel C, Duprey S, Jadwisienczak W, Ingram D, Upadhyay M, David A, Fouchet A, Lüders U and Cardin J. Structural, optical, and electrical properties of $TiO_2$ thin films deposited by ALD: Impact of the substrate, the deposited thickness and the deposition temperature. Appl Surf Sci. 2023; 608, https://doi.org/10.1016/j.apsusc.2022.155214.

22. Kumara S, Tanvi Vats S, Sharma N, and Kumar J. Investigation of annealing effects on $TiO_2$ nanotubes synthesized by a hydrothermal method for hybrid solar cells. Optik - Int J for Light and Electron Optics. 2018; 171 (2018): 492–500

23. El-Nahass, M. M., Soliman, H. S and El-Denglawey, A. Absorption edge shift, optical conductivity, and energy loss function of nano thermal-evaporated N-type anatase $TiO_2$ films. Appl Phys A: Mater Sci Process. 2016; 122 (2016): 775.

24. Hamid AM, Hassan HW and Osman FA. Enhancement of Solar Cell Efficiency by Using TiO2 Nanostructure Doped Fe2O3 Dye and Effect Concentration of Solvent on Optical Properties. AJOPACS. 2019; 7(3):1–14. https://doi.org/10.9734/ajopacs/2019/v7i33009

25. Daughtry J, Abdulrahman S, Alotabi, Howard-Fabretto L, and Andersson, G G.Composition and properties of RF-sputter deposited titanium dioxide thin films,Nanoscale Adv. 2021; 3: 1077-1086

26. Hajjaji A, Amlouk M, Gaidi M, Bessais B, and El Khakani. Chromium Doped TiO2 Sputtered Thin Films: Synthesis, Physical Investigations and Applications. Chromium Doped TiO2 Sputtered Thin Films. 2014;

27. Engberg SLJ, Martinho FM A, Gansukh M, Aguilar Protti A CD, Küngas R, Stamate E, Hansen O, Canulescu S and Schou J. Spin-coated Cu ZnSnS solar cells: A study on the transformation from ink to film. Scientific Reports. 2020; 10: [20749]. https://doi.org/10.1038/s41598-020-77592-z

28. Ahmoum H, Chelvanathan P, Su'ait MS, Boughrara M, Li G, Ali HA, Sopian K, Kerouad M and Amin N. Impact of preheating environment on microstructural and optoelectronic properties of $Cu_2ZnSnS_4$ (CZTS) thin films deposited by spin-coating. Superlattices Microstruct. 2020; 140 (2020) 106452

29. Özdal T, Chtouki T, Kavak H, Figa V,Guichaoua D,Erguig H,Mysliwiec J andBahraoui B. Effect of Annealing Temperature on Morphology and Optoelectronics Properties of Spin-Coated CZTS Thin Films. J InorgPolym Mater 2020; https://doi.org/10.1007/s10904-020-01646-y

30. Abdellatif S, Sharifi P, Kirah K, Ghannam R, Khalil ASG, Erni D, Marlow F. Refractive index and scattering of porous $TiO_2$ films. Microporous and Mesoporous Mater 2018; 264:84-89. doi 10.1016/j.micromeso.2018.01.011.

31. Khan ST and Al-Khedhairy AA. Metals and Metal Oxides: Important Nanomaterials with Antimicrobial Activity. Antimicrobial Nanoarchitectonics. 2017; 195-222. http://dx.doi.org/10.1016/B978-0-323-52733-0.00008-2

32. Lukong V T, Ukoba KO and Jen T C. Analysis of sol aging effects on self-cleaning properties of $TiO_2$ thin film. Mater. Res. Express. 2021; 8 105502. https://doi.org/10.1088/2053-1591/ac2b58

33. Dai M, Guo W, Liu X, Zhang M, Wang Y, Wei L, Hilton G, Hubmayr J, Ullom J, Gao J and Vissers M. Measurement of Optical Constants of TiN and TiN/Ti/TiN Multilayer Films for Microwave Kinetic Inductance Photon-Number-Resolving Detectors. J Low Temp Phys. 2019; 194. 10.1007/s10909-018-2095-9.

34. AL-Jawad SMH, Taha AA and Salim MM. Synthesis and characterization of pure and Fe doped $TiO_2$thin films for antimicrobial activity, Optik. 2017; 142 (2017):42–53.

35. Taha H, Jiang Z, Henry DJ, Amri A, Yin Cand Rahman MM. Improving the optoelectronic properties of titanium-doped indium tin oxide thin films, Semicond. Sci. Technol. 2017; 32: 1-11. https://doi.org/10.1088/1361-6641/aa6e3f

36. Abdullahi S, Momoh M, Moreh AU, Bayawa AM, Hamza B, Argungu GM and Popoola T. Growth Mechanism and Influence of Annealing Temperature on Structural and Compositional Properties of $Cu_2ZnSnS_4$ (CZTS) thin Films Deposited by RF Sputtering Method from a Compound Target, Int J Sci Res Sci Tech. 2017; 3(1):95-82. ISSN 2395-602X. DOI:10.32628/IJSRST17316.

37. Alaya Y, Souissi R, Toumi M, Madani M, El Mir L, Bouguila N and Alaya S. Annealing effect on the physical properties of $TiO_2$thin films deposited by spray pyrolysis. RSC Adv. 2023; 13:21852-21860

38Rajesh K, Narinder A and Navjeet S. Study of Spin Coated Titanium Dioxide Films. Int J Pure Appl Phys. 2017; 13 (1):229-231

39. Zharvan V, Daniyati R, Nur Ichzan NAS, Yudoyono G, Darminto . Study on fabrication of $TiO_2$thin films by spin–coating and their optical properties. AIP Conf. Proc. 2016; 1719, 030018 (2016) https://doi.org/10.1063/1.4943713

40. Hassanien AS and El Radaf IM. Optical characterizations of quaternary Cu2MnSnS4 thin films: Novel synthesis process of film samples by spray pyrolysis technique, Physica B Condens Matter. 2020; 585. https://doi.org/10.1016/j.physb.2020.412110.

41. Dizaji HR, Jamshidi Z A, and Ehsani MH. Effect of thickness on the structural and optical properties of ZnS thin films prepared by flash evaporation technique equipped with modified feeder. Chalcogenide letters. 2011; 8 (4):231-237

42. Abdullahi S, Momoh M, Moreh AU, Bayawa AM, and Saidu A. Synthesis and characterization of CZTS thin films from compound target deposited by RF sputtering method. IOP Conf. Ser.: Mater. Sci. Eng. 2020;805 012001. doi:10.1088/1757-899X/805/1/012001